

PRIMARY RESEARCH

Open Access



pATM and γ H2AX are effective radiation biomarkers in assessing the radiosensitivity of $^{12}\text{C}^{6+}$ in human tumor cells

Jin Zhao^{1*†}, Zhong Guo^{1†}, Shuyan Pei¹, Lei Song¹, Chenjing Wang¹, Jianxiu Ma¹, Long Jin¹, Yanqing Ma¹, Renke He¹, Jianbin Zhong¹, Ying Ma¹ and Hong Zhang²

Abstract

Background: Tumour radiosensitivity would be particularly useful in optimizing the radiation dose during radiotherapy. The aim of the current study was to evaluate the potential value of phosphorylated H2AX (γ H2AX) and ATM (pATM) in assessing $^{12}\text{C}^{6+}$ radiosensitivity of tumour cells.

Methods: Human cervical carcinoma HeLa cells, hepatoma HepG2 cells, and mucoepidermoid carcinoma MEC-1 cells were irradiated with different doses of $^{12}\text{C}^{6+}$. The survival fraction was assayed with clonogenic survival method and the foci of γ H2AX and pATM was visualized using immunocytochemical methods. Flow cytometry was used to assay γ H2AX, pATM and the cell cycle.

Results: The survival fraction decreased immediately in dose-dependent manner, but in turn, significantly increased during 24 h after $^{12}\text{C}^{6+}$ irradiation. Both γ H2AX and pATM foci accumulated linearly with doses and with a maximum induction at 0.5 h for γ H2AX and 0.5 or 4 h for pATM, respectively, and a fraction foci kept for 24 h. The expression of γ H2AX and pATM was in relation to cell cycle. The G0/G1 phase cells had the highest expression of γ H2AX after 0.5 h irradiation and then decreased to a lower level at 24 h after irradiation. An obvious increase of pATM in G2/M phase was shown after 24 h of 2 and 4 Gy irradiation. The significant G2/M phase arrest was shown. There was a close relationship between the clonogenic survival and γ H2AX and pATM expression both in timing and dose in response to $^{12}\text{C}^{6+}$.

Conclusions: The rate of γ H2AX and pATM formation and loss may be an important factor in the response of cells to $^{12}\text{C}^{6+}$. pATM and γ H2AX are effective radiation biomarkers in assessing the radiosensitivity of $^{12}\text{C}^{6+}$ in human tumor cells.

Keywords: $^{12}\text{C}^{6+}$, Human tumor cells, Survival fraction, γ H2AX, ATM

Background

Radiation-induced cell death is mediated through induction of double-strand breaks (DSB) in DNA, which are lethal to cells if not repaired [1]. The energy deposition by low-linear energy transfer (LET) radiation is distributed randomly throughout the cell, whereas the energy from high-linear energy transfer (LET) radiation is deposited

as discrete tracks where the particle has passed through the cell [2]. As a result, the DNA damage induced by high-LET heavy ion radiation is more complex than that by X- or gamma rays and leads to more severe biological consequences [3]. Although these effects can lead to cell death, mutations, genomic instability, or carcinogenesis, problems associated with the repair of the high-LET induced DSB are not fully understood.

Mammalian cells repair these lesions principally through two separate pathways: homologous recombination (HR), which is thought to rely on the presence of an intact sister chromatid during the S and G2 phases, and

*Correspondence: gz6768@163.com

[†]Jin Zhao and Zhong Guo contributed equally to this work

¹ Medical College of Northwest Minzu University, Lanzhou 730030, People's Republic of China

Full list of author information is available at the end of the article

nonhomologous end joining (NHEJ), which utilizes DNA repair protein and is thought to predominate in the G1 phase. The NHEJ pathway, however, is regarded as the major pathway for the repair of radiation induced DSB in mammalian cells [4]. Activation of the Ataxia Telangiectasia Mutation (ATM) through its phosphorylation on Ser1981 (ATM-S1981P, pATM), and phosphorylation of one of the variants of histone H2AX, histone H2AX on Ser139 (γ H2AX), not only are the main participants, but also the early markers of a cell's response to DNA damage, particularly if the damage involves formation of DSB [5, 6]. These modifications of ATM and H2AX trigger pathways are involved in DNA repair and in activating checkpoints that halt progression through the cell cycle [7, 8]. The pause in cell cycle progression is needed to allow for DNA repair to succeed prior to resumption of DNA replication or cell division.

High linear energy transfer (LET) radiation, such as heavy ion particles, is believed to produce high yields of clustered DNA damage including DSB [9–11]. A prolonged cell cycle arrest [12] and a slower rejoining of DSB [13] have been reported to occur after exposure to high-LET radiation. However, the repair dynamics of high-LET radiation-induced DNA damage remains poorly understood.

In the present study, the expression of γ H2AX and pATM were assayed with immunocytochemical and flow cytometry methods and the correlation between clonogenic survival and the level of γ H2AX and pATM was evaluated in human cervical carcinoma HeLa cells, hepatoma HepG2 cells and mucoepidermoid carcinoma MEC-1 cells after irradiation with $^{12}\text{C}^{6+}$. Our studies emphasize the rate of γ H2AX and pATM formation and loss may be an important factor in the response of cells to $^{12}\text{C}^{6+}$. pATM and γ H2AX are effective radiation biomarkers in assessing the radiosensitivity of $^{12}\text{C}^{6+}$ in human tumor cells.

Methods

Cell lines

Human cervical carcinoma HeLa cell and human hepatoma HepG2 cells were purchased from the Shanghai Institute of Biochemistry and Cell Biology, Shanghai, China. Human mucoepidermoid carcinoma MEC-1 cells were purchased from the School of Stomatology, at the Fourth Military Medical University of Xian, China. The cells were subcultured in Dulbecco's Modified Eagle Medium (DMEM) (GIBCO, USA), containing 10% newborn calf serum, 100 U/mL penicillin, 125 g/mL streptomycin, and 0.03% glutamine.

Irradiation using carbon ion beams

Exponentially growing cells seeded at 2×10^4 cells/100 mm dish were exposed to different dosages of

$^{12}\text{C}^{6+}$. Immediately following irradiation, the medium was quickly removed and cells were incubated for various time intervals at 37 °C before harvest. $^{12}\text{C}^{6+}$ was supplied by the Heavy Ion Research Facility in Lanzhou (HIRFL) at the Institute of Modern Physics, Chinese Academy of Sciences (IMP-CAS). Since the energy decays through the vacuum window, air gap, Petri dish cover and medium, the energy of the ion beams on cell samples was adjusted to be 300 meV/u, corresponding to a LET of 15 keV/ μm and the dose rate was adjusted to be about 0.4 Gy/min. The ion beams were calibrated using an absolute ionization chamber. The tumor cells were irradiated by plateau of carbon ions LET curve and the dose of scatter off the walls of the plate has been calculated and incorporated into the total dose. The data (preset numbers converted to absorbed dose of particle radiation) was automatically obtained using a microcomputer during irradiation. The dose rate was approximately 1.38 Gy/min and the dose used for $^{12}\text{C}^{6+}$ irradiation was 0.5, 1, 2 and 4 Gy.

Clonogenic survival assays

The cells were cultured for 0.5, 4 and 24 h after irradiation and then were washed with phosphate-buffered saline, trypsinized, and counted using a Coulter counter, replated at a density of 5×10^2 – 3×10^4 cells in duplicate using 100 mm dishes for cell-survival assays. Plates were stained and colonies were counted two weeks later. Counts from the two plates were averaged, and surviving fraction was calculated as the ratio of the plating efficiency of the treated cells divided by the plating efficiency of the control cells. Experiments were repeated 3–4 times [14]. The survival fraction was calculated using the following formula:

Survival fraction

$$= \frac{\text{No. of colonies}}{\text{No. of cells plating} \times (\text{plating efficiency}/100)} \quad (1)$$

Immunofluorescence microscopy for γ H2AX and pATM foci

Immunofluorescent microscopy was conducted according to previously reported procedures with modifications [15, 16]. Briefly, 2×10^4 cells were seeded onto 35 mm dishes containing a glass cover slip in each well. After irradiation, slides were air-dried, and fixed for 0.5 h in 2% paraformaldehyde in TBS. Cells were rinsed in TBS, placed in -20 °C methanol for 1 min, rinsed, then placed for 20 min in TBS plus 1% bovine serum albumin and 0.2% Tween-20 (TTN) and finally incubated for 2 h with anti-phospho-histone H2AX (Ser-139) mAb (Upstate, Lake Placid, NY), anti-phospho-ATM (ser1981) mAb (Upstate, Lake Placid, NY), both diluted to 1:500 in TTN. Slides were washed and incubated with FITC-conjugated anti-mouse goat F(ab')₂ fragment (DAKO, Carpinteria,

CA) diluted 1:200 in TTN and FITC-conjugated anti-rabbit goat F(ab')₂ fragment (DAKO, Carpinteria, CA) diluted 1:200 in TTN for 1 h at room temperature. Slides were rinsed and then immersed in 0.05 mg/mL DAPI for 15 min, rinsed and mounted with cover slips using 10 μ L Fluorogard (Bio-Rad) as the antifade mounting medium, and sealed. To prevent bias in selection of cells that display foci, over 800 randomly selected cells were counted. Cells with three or more foci of any size were classified as positive. All experiments were repeated in triplicate.

Flow cytometry assay for γ H2AX and pATM

Flow cytometry analysis was conducted as previously described [17, 18]. After the various treatments, cells were fixed with cold 70% methanol and kept at -20°C for up to 2 weeks until further analysis. Cells were centrifuged and rinsed with PBS, blocked with PST (4% fetus bovine serum in PBS) for 15 min at room temperature and rinsed a second time with PBS. Cells were first incubated with Anti-phospho-Histone H2AX (Ser139) mAb (Upstate, Lake Placid, NY) and Anti-phospho-ATM (ser1981) mAb (Upstate, Lake Placid, NY) at 1:300 and 1:100 dilution for 2 h at room temperature, then rinsed with PBS and incubated with Alexa Fluor 488-conjugated AffiniPure Goat Anti-Mouse IgG (H + L) at a 100- and 200-fold dilution for another 1 h at room temperature and rinsed again in PBS. Cells were further incubated for 0.5 h at room temperature with 50 $\mu\text{g}/\text{mL}$ PI. Cells were filtered through a 35 μm pore strainer and were analyzed using a flow cytometer (Becton–Dickinson, Bedford, MA, USA). Cell cycle analysis was conducted as described by Amrein et al. [19].

To examine the relationship between the expression of γ H2AX and pATM in each phase of the cell cycle, the changes in γ H2AX and pATM immunofluorescence intensity (IF) were calculated in each phase of the cycle by gating

G1, S and G2/M cells based on differences in DNA content. The means of γ H2AX and pATM and positive ratios for G1, S and G2/M populations of cells in the DMSO control groups were subtracted from the respective means of the non-irradiated cells. After this subtraction, the irradiation-induced changes in positive γ H2AX and pATM ratio were obtained. Data is presented as the mean of the γ H2AX and pATM positive ratios of each cell cycle compartment. All experiments were performed three times.

Statistical analysis

SPSS version 18.0 software (SPSS Inc., Chicago, Illinois, USA) was used for the statistical analysis. Data are expressed as mean \pm standard deviation (SD). A two-tailed Student's t test was performed to assess the differences between any two groups. The significance of the correlation coefficient was also calculated. A value of $P < 0.05$ was considered statistically significant. Statistical inferences were based on two-sided tests at a significance level of $P < 0.05$.

Results

Growth dynamics of colony survival assay

Clonogenics cells were inactivated immediately, but in turn, significantly increased during 24 h after $^{12}\text{C}^{6+}$ irradiation ($P < 0.05$). The survival fraction decreased in dose-dependent manner at every time point for each tumor cells ($P < 0.05$, Fig. 1).

Immunofluorescence staining of phosphorylated H2AX and ATM foci

Phosphorylated H2AX and ATM foci were observed with anti- γ H2AX antibodies (green), anti-ATMpSer1981 antibodies (green) and the nuclei were stained with DAPI (blue). Typical images of $^{12}\text{C}^{6+}$ induced γ H2AX and pATM foci are shown in Fig. 2. After 0.5 h of radiation,

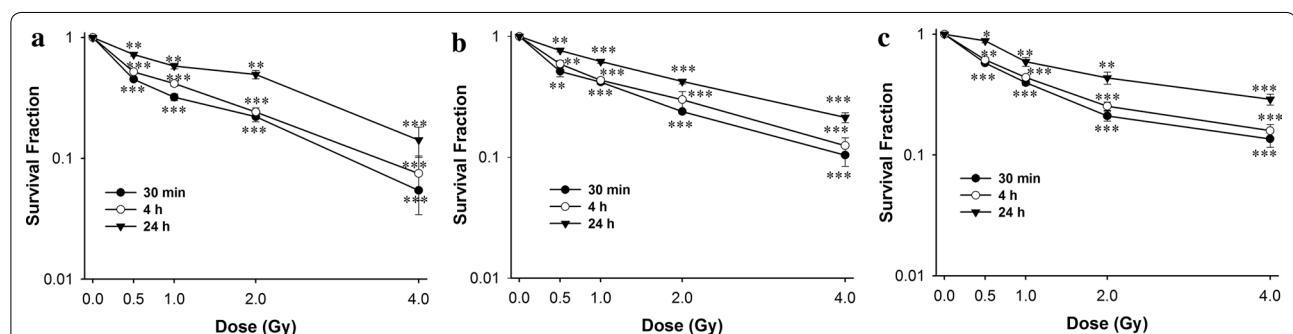
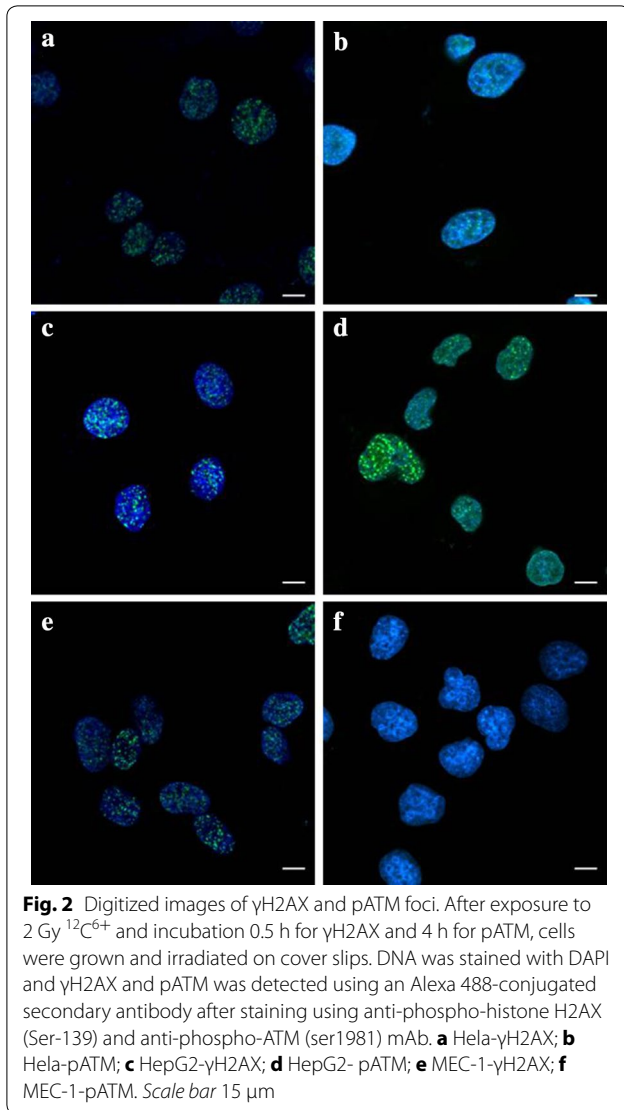


Fig. 1 A survival curve for the HeLa, HepG2 and MEC-1 cell lines, as determined by clonogenic assay. Exponentially growing cells were plated and irradiated, the cells were taken at the indicated time intervals after irradiation of $^{12}\text{C}^{6+}$ and a clonogenic assay was performed. The means and SD are shown for three independent experiments with 3 replicates in each experiment. Untreated cells served as a control. After incubation for two weeks, colonies with cells greater than 50 were counted. **a** HeLa cells; **b** HepG2 cells; **c** MEC-1 cells. * $P < 0.05$, ** $P < 0.01$, *** $P < 0.001$ vs. 0 Gy irradiation



γ H2AX and pATM foci, visualized as bright spots, were present in all cells. The time and dose dependent induction of γ H2AX and pATM foci by $^{12}\text{C}^{6+}$ were counted in all tumor cell lines. It was noted that the strongest inductions of γ H2AX foci were at 0.5 h for all three tumor cell lines. However, the strongest induction of pATM foci was at 4 h for HeLa and HepG2 cells and at 0.5 h for MEC-1 cells, and then decreased over time. A fraction foci persisted for at least 24 h for γ H2AX and pATM for all three tumor cells, for example, about 62.2–83.8% γ H2AX foci and 80.7–100% pATM foci were shown in three cell lines after 4 Gy radiation (Fig. 3).

$^{12}\text{C}^{6+}$ induces H2AX and ATM phosphorylation in a cell cycle-dependent manner

In order to further determine the phosphorylation levels of H2AX and ATM, the intensity of γ H2AX and pATM

were assayed with flow cytometry. Typical flow cytometry histograms of $^{12}\text{C}^{6+}$ induced phosphorylation of H2AX and ATM in a cell cycle-dependent manner are shown in Fig. 4.

After 0.5 and 4 h irradiation, the percentage of γ H2AX positive cells increased in a dose dependent manner in almost all phases, in which, G0/G1 phase cells had the highest expression of γ H2AX after 0.5 h irradiation and then decreased to a lower level at 24 h after irradiation (Fig. 5). An obvious increase of pATM in G2/M was shown after 24 h of 2 and 4 Gy irradiation (Fig. 6).

The effect of the cell cycle of the three tumor cell lines for $^{12}\text{C}^{6+}$ exposure is presented in Fig. 7. There was a significant G2/M phase arrest. For example, after 4 Gy irradiation, there were 40.5% HeLa cells in G2/M after 24 h vs. 17.8% in G2/M after 0.5 h and there were about 25.0 and 51.9% of HepG2 and MEC-1 cells in G2/M after 24 h vs. 17.9 and 17.6% in G2/M after 0.5 h.

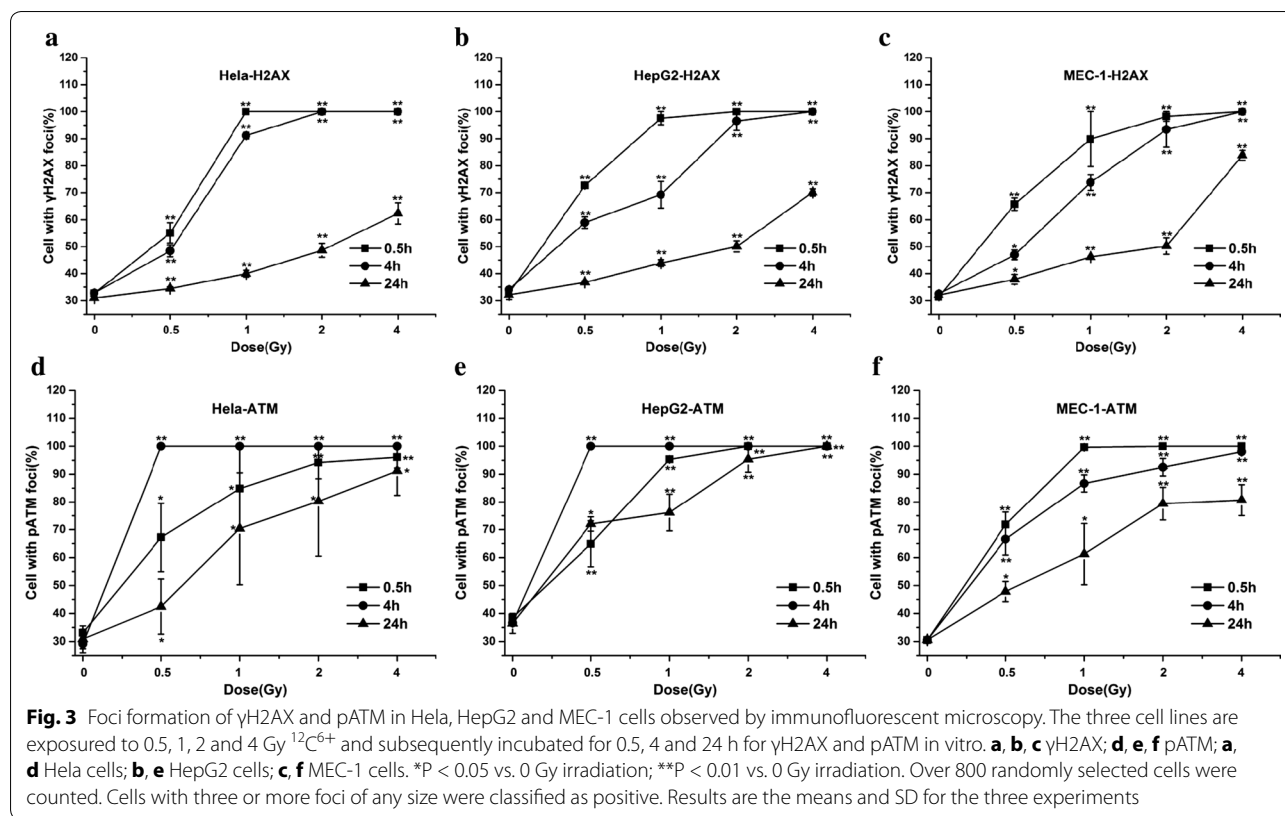
The correlation between the clonogenic survival and γ H2AX and pATM foci in $^{12}\text{C}^{6+}$ irradiated tumor cells

In order to determine if there was a direct quantitative relationship between the clonogenic survival and γ H2AX and pATM expression, cells were exposed to different dose $^{12}\text{C}^{6+}$ and incubated to different time. A positive correlation was shown between the clonogenic survival and γ H2AX and pATM foci. The correlation coefficients for almost all parameters we used, such as different doses and irradiated time points, were statistically significant ($P < 0.05$, Tables 1, 2) suggesting that these two variables are directly linked.

Discussion

In the present study, radiosensitivities of different tumour cell lines to $^{12}\text{C}^{6+}$ were established using the clonogenic assay. We selected three tumor cell lines which were of different tissue origins. The different cell types were used to ensure that the assay was able to distinguish the radiosensitivity across different tumor types. In the clonogenic assay, a significantly survival inhibition was shown in $^{12}\text{C}^{6+}$ irradiation over time and dose (Fig. 1). It, therefore, seemed reasonable to conclude that an early significant increase in the survival fraction within 24 h occurred after $^{12}\text{C}^{6+}$ irradiation.

A cytological manifestation of nuclear activity in response to ionizing radiation (IR) is the formation of the so-called IR-induced foci (IRIF) [20]. IRIFs are dynamic, microscopically discernible structures containing thousands of copies of proteins, including γ H2AX, ATM, CHK2, p53 and MRE11/RAD50/NBS1 (MRN) complex, which accumulate in the vicinity of a DSB [21, 22]. Phosphorylation of histone H2AX is among the earliest changes to occur at sites of DSB damage, where it



is thought to facilitate repair through maintaining structural changes in chromatin. γ H2AX induction following exposure to IR is reported to be mediated by ATM and DNA-PK [23]. The phosphorylation of H2AX by ATM occurs at sites of DSB in the cell nucleus whereas ATM autophosphorylation is thought to take place throughout the nucleoplasm. The figures shown here provide a visualization of $^{12}\text{C}^{6+}$ ion tracks inside nuclei in human cells by utilizing immunocytochemical methods with antibodies recognizing γ H2AX and pATM (Fig. 2). This assay is quite sensitive and is a specific indicator for the existence of a DSB [24–26].

In the present study, we firstly compared the background values of γ H2AX and pATM in three tumor cell lines. The expression of endogenous γ H2AX and pATM foci was lower and there was not a significant difference between the three tumor cell lines we used ($P > 0.05$). We, then, measured foci frequency for up to 24 h and found that a fraction of foci persisted for at least 24 h after high LET carbon ions radiation (Fig. 3). This confirms the earlier studies that these persistent γ H2AX and pATM foci as evidence of persistent DSB.

Then we confirmed the induction of DSB as measured by γ H2AX and pATM signaling in three cell lines occurs in a dose-dependent manner, as expected, but that foci formation and resolution is different (Fig. 3). The highest

level of γ H2AX and pATM foci presence in $^{12}\text{C}^{6+}$ irradiated cells at 0.5 h or 4 h after irradiation indicates the repair of damage began early in tumor cells. γ H2AX foci resolution in MEC-1 cells were seemingly delayed and incomplete compared to the other two cell lines because MEC-1 cells expressed higher levels of γ H2AX foci even 24 h after 4 Gy irradiation. HepG2 cells had the highest levels of pATM foci at 24 h after 2 and 4 Gy irradiation, so pATM foci resolution in HepG2 cells is also delayed and incomplete compared to other two cells. The data presented here suggest that, presumably as a result of loss of function in some aspects of DNA repair, MEC-1 cells are slowest to repair and are left with more residual damage than the other two tumor cells, as measured by γ H2AX foci resolution. When measured by pATM foci resolution HepG2 cells are also slower to repair than the other two cell lines. Of course, foci resolution is not an exact measurement of repair kinetics; recent data suggest that dephosphorylation of H2AX occurs with a significant lag after DSB repair, following protein dissociation from chromatin. Interestingly, this dephosphorylation event may promote checkpoint recovery [27]. In a word, in the present study the higher activation of ATM shown at 4 h compared with H2AX phosphorylation at 0.5 h and γ H2AX and pATM foci delayed resolution in MEC-1 and HepG2 cells maybe highlight signaling differences with

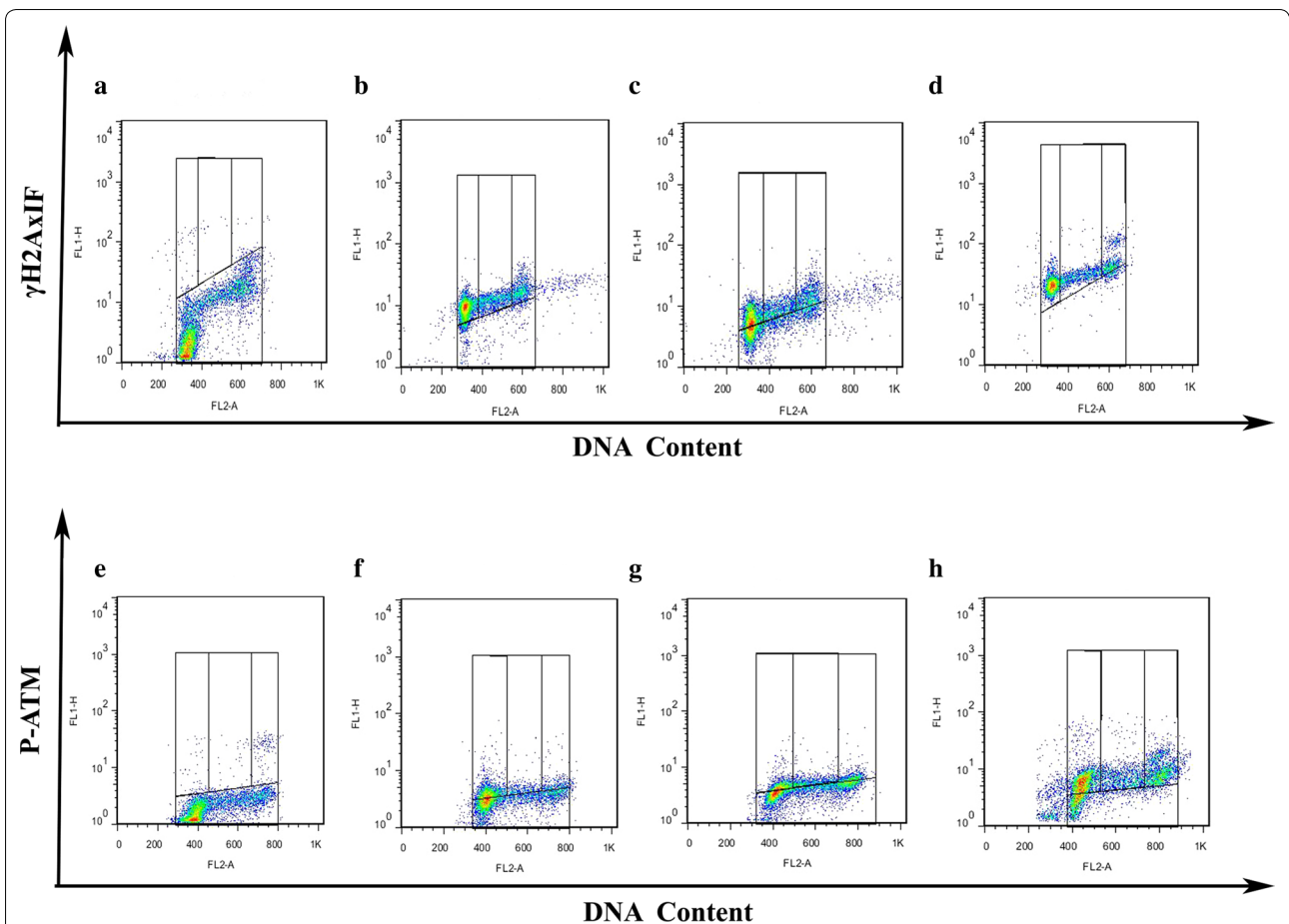


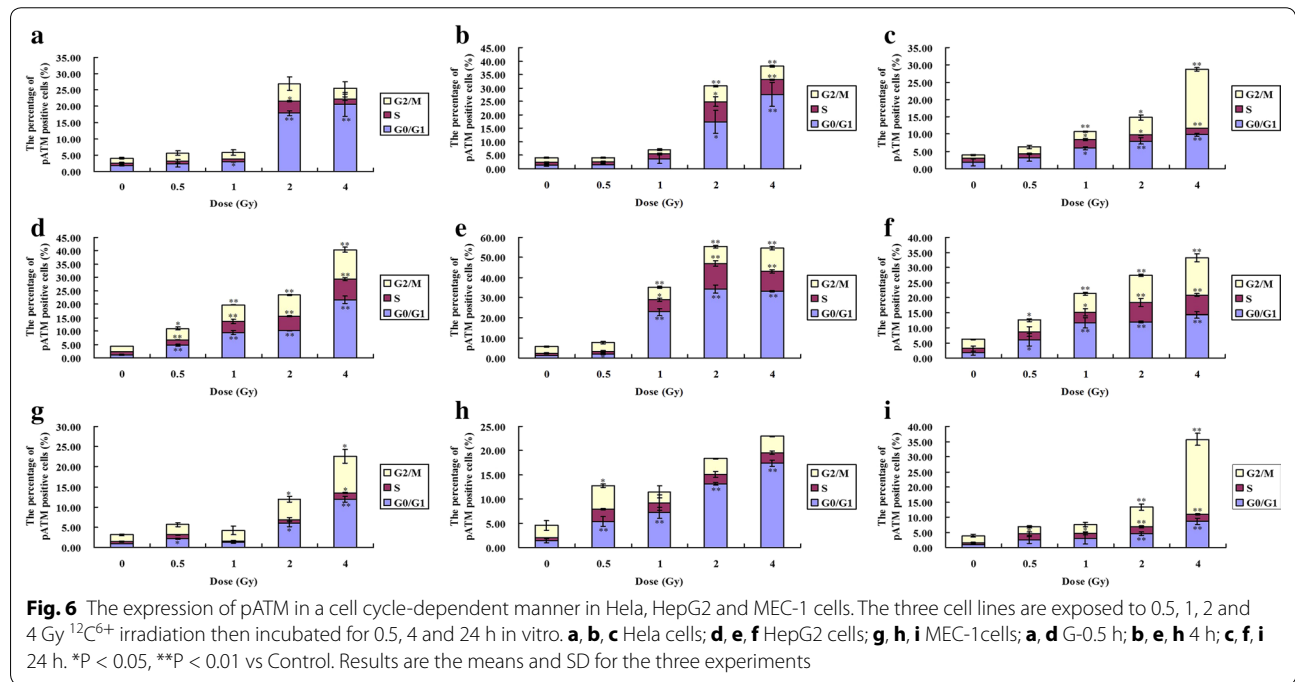
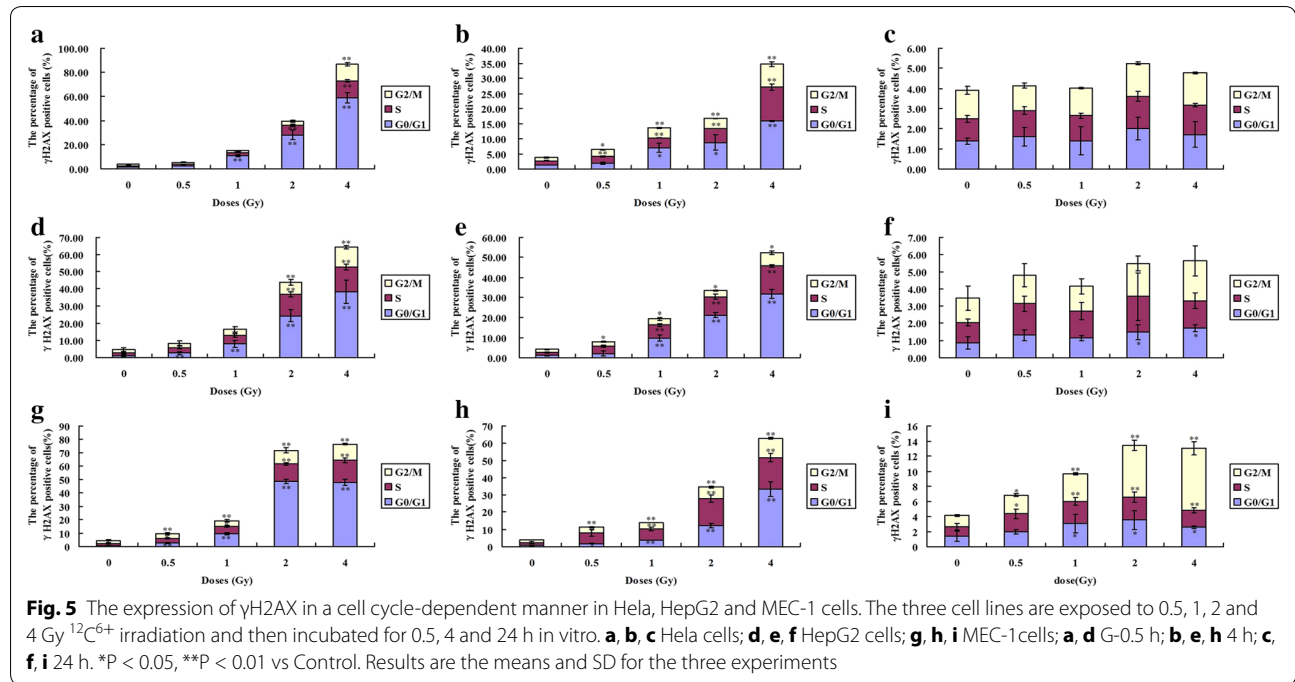
Fig. 4 γ H2AX and pATM in a cell cycle-dependent manner in HeLa, HepG2 and MEC-1 cells. Bivariate (γ H2AX and pATM IF vs DNA content) distributions of control and 4 Gy $^{12}\text{C}^{6+}$ irradiation and subsequent incubation for 0.5 h for γ H2AX and 4 h for phosphorylated ATM in vitro. **a, b, c, d** γ H2AX; **e, f, g, h** pATM; **a, e** Control (HeLa cells); **b, f** HeLa cells; C,G-HepG2 cells; **d, h** MEC-1 cells

respect to clustered damage. Concurrent activation of ATM and γ H2AX suggest that the latter event, at least in part, was independent in ATM.

In order to further determine the phosphorylation levels of H2AX and ATM, the intensity of γ H2AX and pATM were assayed with flow cytometry. Our result proved the expression of γ H2AX and pATM was in relation to cell cycle. Flow cytometry, which is a convenient method for detecting differences in γ H2AX and pATM antibody binding in populations of cells, offers the advantage of measuring change in γ H2AX and pATM intensity in relation to the cell cycle position [28–30]. Olive PL assessed the expression of γ H2AX phosphorylation by flow cytometry to detect and measure DNA damage induced by X-rays. It has also been reported that cytometric assessment of γ H2AX fluorescence decay in blood cells of X-irradiated patients and low and high LET radiated cells offers a sensitive measure of DNA damage in vivo and in vitro [31]. Flow cytometry also offers the advantage of measuring changes in phosphorylated

ATM intensity in relation to cell cycle position in mitogenic stimulated lymphocytes and glucose antimetabolite 2-deoxy-D-glucose (2-DG) treated B-lymphoblastoid TK6 cells [32, 33]. Analysis of the post-irradiation kinetics of γ H2AX and pATM fluorescence with flow cytometry revealed a pattern which suggests that G0/G1,S and G2/M phase cells vary independently on the relative expression of γ H2AX and pATM. The present study demonstrates that G0/G1 phase cells are more uniformly affected than S and G2/M phase cells. For example, at 0.5 h after 4 Gy $^{12}\text{C}^{6+}$ irradiation, over 40% of G0/G1 phase cells had increased expression of γ H2AX and a little decrease was shown at 4 h after irradiation in all three cell lines (Fig. 5). Although G0/G1 phase cells had increased expression of pATM, interesting, the G2/M cells showed a significantly increase of pATM at 24 h after 2 and 4 Gy $^{12}\text{C}^{6+}$ irradiation (Fig. 6).

Tumor cells used here show no significant G1 checkpoint response after irradiation [33]. However, the data presented here demonstrates a clear dose response G2



checkpoint that prolongs the G2 phase by several hours even after very low radiation doses (Fig. 7). These data imply that the tumor cells used here are relatively more dependent on the G2 checkpoint to facilitate repair. Others have recently described this phenotype in other

tumor cell lines and demonstrated that it predicts sensitivity to G2 checkpoint inhibition [34].

The results of the γ H2AX and pATM expression were compared with those of clonogenic assay in determining the radiosensitivity of the tumour cell lines. For the

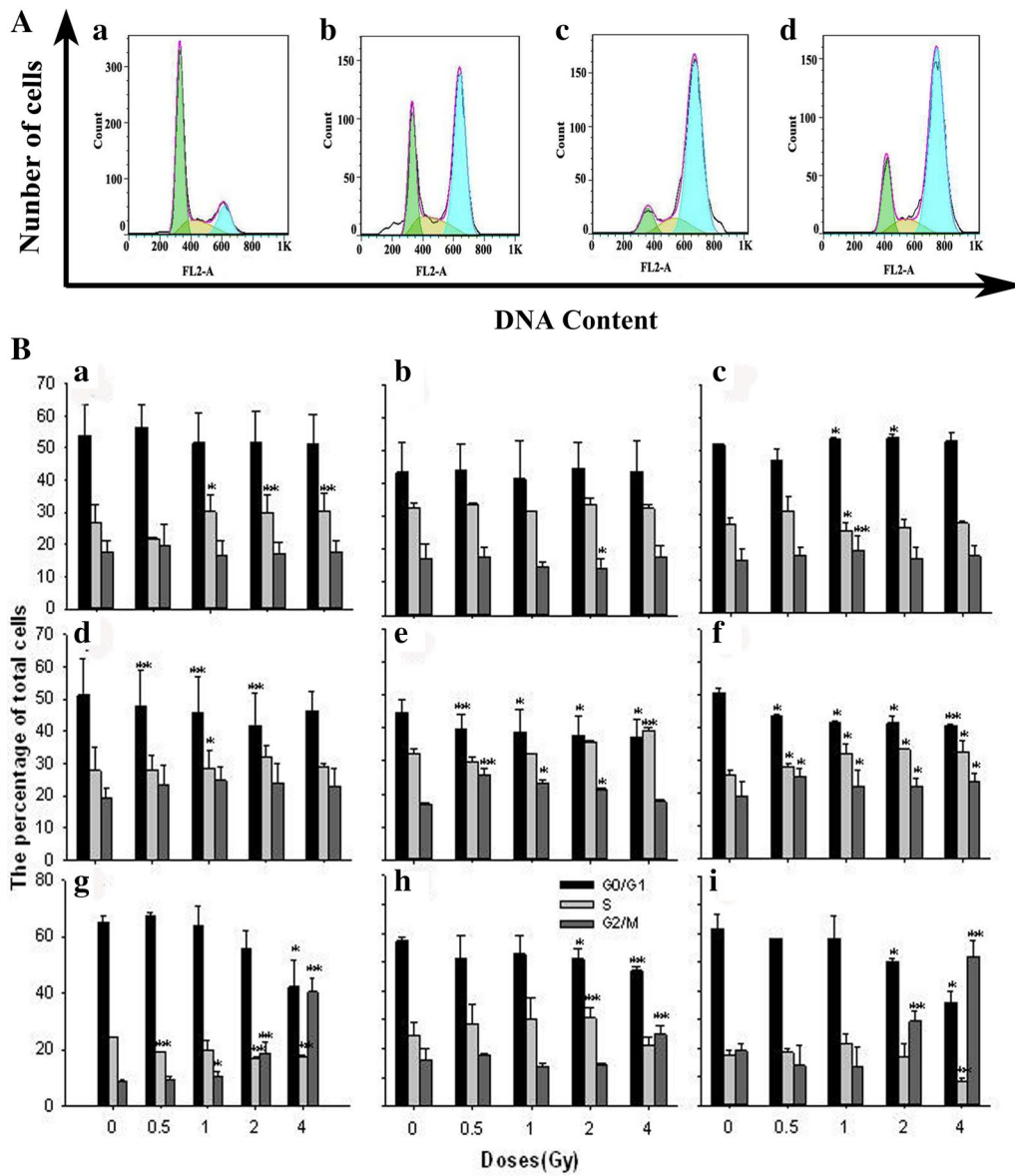


Fig. 7 **A** Cell cycle distribution of three cell lines. *a*-HeLa, HepG2 and MEC-1 cell are treated with 4 Gy $^{12}\text{C}^{6+}$ followed incubation for 24 h. *a* Control (HeLa cells), *b* HeLa cells, *c* HepG2 cells, *d* MEC-1 cells. **B** Three cell lines treated with 0.5, 1, 2 and 4 Gy $^{12}\text{C}^{6+}$ irradiation and subsequently incubated for 0.5, 4 and 24 h. *a, b, c* 0.5 h; *d, e, f* 4 h; *g, h, i* 24 h. *a, d, g* HeLa cells; *b, e, h* HepG2 cells; *c, f, i* MEC-1 cells. * $P < 0.05$, ** $P < 0.01$ vs Control. Results are the means and SD for the three experiments

Table 1 Correlation coefficient obtained from γH2AX by correlating expression with the SF

	0.5 h		4 h		24 h	
	r values	P values	r values	P values	r values	P values
HeLa	-0.91	0.03	-0.906	0.03	-0.964	<0.01
HepG2	-0.954	0.01	-0.978	<0.01	-0.955	0.01
MEC-1	-0.988	<0.01	-0.969	0.01	-0.879	0.05

Table 2 Correlation coefficient obtained from pATM by correlating expression with the SF

	0.5 h		4 h		24 h	
	r values	P values	r values	P values	r values	P values
Hela	-0.984	<0.01	-0.875	0.05	-0.943	0.02
HepG2	-0.944	0.02	-0.856	0.06	-0.955	0.01
MEC-1	-0.962	0.01	-0.986	<0.01	-0.976	<0.01

three cell lines, the DNA repair kinetics after $^{12}\text{C}^{6+}$ irradiation, as measured using γH2AX and pATM foci assay, were strongly correlated with the radiosensitivity of clonogenicity, which is in agreement with our former report [14], in which we proved γH2AX foci assay had the potential value in assessing the radiosensitivity of carbon beam in human tumor cell lines.

Conclusion

Our result suggests the rate of γH2AX and pATM formation and loss may be an important factor in the response of cells to $^{12}\text{C}^{6+}$. pATM and γH2AX are effective radiation biomarkers in assessing the radiosensitivity of $^{12}\text{C}^{6+}$ in human tumor cells.

Abbreviations

DMEM: Dulbecco's modified Eagle's medium; PI: propidium iodide; DMSO: dimethyl sulfoxide; γH2AX : H2AX phosphorylation; ATM: Ataxia telangiectasia-mutated; DNA-PK: DNA dependent protein kinase; MRN: MRE11/RAD50/NBS; DSB: DNA double strand breaks; NHEJ: non-homologous end-joining; HR: homologous recombination; IRIF: IR-induced foci.

Authors' contributions

JZ was project manager, JZ, ZG and HZ was project manager and wrote most of the article. LS, LJ and JM was principal investigator of this Flow cytometry assay, CW, YM and SP was principal investigator of this Immunofluorescence microscopy, RH, JZ and CR was principal investigator of this Cell culture and treatment. All authors read and approved the final manuscript.

Author details

¹ Medical College of Northwest Minzu University, Lanzhou 730030, People's Republic of China. ² Department of Radiation Medicine, Institute of Modern Physics, Chinese Academy of Science, Lanzhou 730030, People's Republic of China.

Acknowledgements

This work was supported in part by Grants from the National Natural Science Foundation of China (Nos. 31060127, 81260442, 81560508 and 31560254) and Key Program of the National Natural Science Foundation of China (U1432248) and Program for Leading Talent of SEAC ([2016]57) and National Undergraduate Training Programs for Innovation and Entrepreneurship (201610742002).

Competing interests

The authors declare that they have no competing interests.

Availability of data and materials

Data sharing not applicable to this article as no datasets were generated or analysed during the current study.

Funding

Fund of the National Natural Science Foundation of China (Nos. 31060127, 81260442, 81560508 and 31560254) and Key Program of the National Natural

Science Foundation of China (U1432248) and Program for Leading Talent of SEAC ([2016]57) and National Undergraduate Training Programs for Innovation and Entrepreneurship (201610742002).

Publisher's Note

Springer Nature remains neutral with regard to jurisdictional claims in published maps and institutional affiliations.

Received: 4 January 2017 Accepted: 20 April 2017

Published online: 26 April 2017

References

- Okayasu R. Repair of DNA damage induced by accelerated heavy ions—a mini review. *Int J Cancer*. 2012;130:991–1000.
- Lorat Y, Brunner CU, Schanz S, et al. Nanoscale analysis of clustered DNA damage after high-LET irradiation by quantitative electron microscopy—the heavy burden to repair. *DNA Repair (Amst)*. 2015;28:93–106.
- Takahashi M, Hirakawa H, Yajima H, et al. Carbon ion beam is more effective to induce cell death in sphere-type A172 human glioblastoma cells compared with X-rays. *Int J Radiat Biol*. 2014;90:1125–32.
- Gerelchuluun A, Manabe E, Ishikawa T, et al. The major DNA repair pathway after both proton and carbon-ion radiation is NHEJ, but the HR pathway is more relevant in carbon ions. *Radiat Res*. 2015;183:345–56.
- Horn S, Brady D, Prise K. Alpha particles induce pan-nuclear phosphorylation of H2AX in primary human lymphocytes mediated through ATM. *Biochim Biophys Acta*. 2015;1853((10 Pt A)):2199–206.
- Meyer B, Voss KO, Tobias F, et al. Clustered DNA damage induces pan-nuclear H2AX phosphorylation mediated by ATM and DNA-PK. *Nucleic Acids Res*. 2013;41:6109–18.
- Turinetto V, Giachino C. Multiple facets of histone variant H2AX: a DNA double-strand-break marker with several biological functions. *Nucleic Acids Res*. 2015;43:2489–98.
- Larsen DH, Stucki M. Nucleolar responses to DNA double-strand breaks. *Nucleic Acids Res*. 2016;44:538–44.
- Lorat Y, Timm S, Jakob B, et al. Clustered double-strand breaks in heterochromatin perturb DNA repair after high linear energy transfer irradiation. *Radiother Oncol*. 2016;121:154–61.
- Nickoloff JA. Photon, light ion, and heavy ion cancer radiotherapy: paths from physics and biology to clinical practice. *Ann Transl Med*. 2015;3(21):336.
- Xue L, Furusawa Y, Okayasu R, et al. The complexity of DNA double strand break is a crucial factor for activating ATR signaling pathway for G2/M checkpoint regulation regardless of ATM function. *DNA Repair (Amst)*. 2015;25:72–83.
- Xue L, Furusawa Y, Yu D. ATR signaling cooperates with ATM in the mechanism of low dose hypersensitivity induced by carbon ion beam. *DNA Repair (Amst)*. 2015;34:1–8.
- Xue L, Yu D, Furusawa Y, et al. Regulation of ATM in DNA double strand break repair accounts for the radiosensitivity in human cells exposed to high linear energy transfer ionizing radiation. *Mutat Res*. 2009;670:15–23.
- Zhao J, Guo Z, Zhang H, et al. The potential value of the neutral comet and γH2AX foci assays in assessing radiosensitivity to carbon ion beams radiation therapy in human tumor cell lines. *Radiol Oncol*. 2013;47:247–57.

15. Banuelos CA, Banáth JP, MacPhail SH, et al. Radiosensitization by the histone deacetylase inhibitor PCI-24781. *Clin Cancer Res*. 2007;13(22 Pt 1):6816–26.
16. Takahashi A, Yamakawa N, Kirita T, et al. DNA damage recognition proteins localize along heavy ion induced tracks in the cell nucleus. *J Radiat Res*. 2008;49:645–52.
17. Schmid TE, Dollinger G, Beisker W, et al. Differences in the kinetics of gamma-H2AX fluorescence decay after exposure to low and high LET radiation. *Int J Radiat Biol*. 2010;86:682–91.
18. Guo Z, Zhao J, Song L, et al. Induction of H2AX phosphorylation in tumor cells by gossypol acetic acid is mediated by phosphatidylinositol 3-kinase (PI3 K) family. *Cancer Cell Int*. 2014;14:141.
19. Loignon M, Amrein L, Dunn M, Aloyz R. XRCC3 depletion induces spontaneous DNA breaks and p53-dependent cell death. *Cell Cycle*. 2007;6:606–11.
20. Maser RS, Monsen KJ, Nelms BE, Petrini JH. hMre11 and hRad50 nuclear foci are induced during the normal cellular response to DNA double-strand breaks. *Mol Cell Biol*. 1997;17:6087–96.
21. Siddiqui MS, François M, Fenech MF, Leifert WR. γ H2AX responses in human buccal cells exposed to ionizing radiation. *Cytom A*. 2015;87:296–308.
22. Bekker-Jensen S, Lukas C, Kitagawa R, et al. Spatial organization of the mammalian genome surveillance machinery in response to DNA strand breaks. *J Cell Biol*. 2006;173:195–206.
23. Nambiar DK, Rajamani P, Deep G, et al. Silibinin preferentially radiosensitizes prostate cancer by inhibiting DNA repair signaling. *Mol Cancer Ther*. 2015;14:2722–34.
24. Rogakou EP, Boon C, Redon C, Bonner WM. Megabase chromatin domains involved in DNA double-strand breaks in vivo. *J Cell Biol*. 1999;146:905–16.
25. Osipov AN, Pustovalova M, Grekhova A, et al. Low doses of X-rays induce prolonged and ATM-independent persistence of γ H2AX foci in human gingival mesenchymal stem cells. *Oncotarget*. 2015;6:27275–87.
26. Nakajima NI, Brunton H, Watanabe R, et al. Visualisation of γ H2AX foci caused by heavy ion particle traversal; distinction between core track versus non-track damage. *PLoS ONE*. 2013;8:e70107.
27. Keogh MC, Kim JA, Downey M, et al. A phosphatase complex that dephosphorylates gammaH2AX regulates DNA damage checkpoint recovery. *Nature*. 2006;439:497–501.
28. MacPhail SH, Banáth JP, Yu Y, et al. Expression of phosphorylated histone H2AX in cultured cell lines following exposure to X-rays. *Int J Radiat Biol*. 2003;79:351–8.
29. MacPhail SH, Banáth JP, Yu Y, et al. Cell cycle-dependent expression of phosphorylated histone H2AX: reduced expression in unirradiated but not X-irradiated G1-phase cells. *Radiat Res*. 2003;159:759–67.
30. Yu T, MacPhail SH, Banáth JP, et al. Endogenous expression of phosphorylated histone H2AX in tumors in relation to DNA double-strand breaks and genomic instability. *DNA Repair (Amst)*. 2006;5:935–46.
31. Ismail IH, Wadhra TI, Hammarsten O. An optimized method for detecting gamma-H2AX in blood cells reveals a significant interindividual variation in the gamma-H2AX response among humans. *Nucleic Acids Res*. 2007;35:e36.
32. MacPhail SH, Banáth JP, Yu Y, et al. Cell cycle-dependent expression of phosphorylated histone H2AX: reduced expression in unirradiated but not X-irradiated G1-phase cells. *Radiat Res*. 2003;159:759–67.
33. Tanaka T, Kurose A, Halicka HD, et al. 2-deoxy-D-glucose reduces the level of constitutive activation of ATM and phosphorylation of histone H2AX. *Cell Cycle*. 2006;5:878–82.
34. Chen Z, Xiao Z, Gu WZ, et al. Selective Chk1 inhibitors differentially sensitize p53-deficient cancer cells to cancer therapeutics. *Int J Cancer*. 2006;119:2784–94.

Submit your next manuscript to BioMed Central
and we will help you at every step:

- We accept pre-submission inquiries
- Our selector tool helps you to find the most relevant journal
- We provide round the clock customer support
- Convenient online submission
- Thorough peer review
- Inclusion in PubMed and all major indexing services
- Maximum visibility for your research

Submit your manuscript at
www.biomedcentral.com/submit

